

Selective visual detection of Pb(II) ion via gold nanoparticles coated with a dithiocarbamate-modified 4'-aminobenzo-18-crown-6

Vaibhavkumar N. Mehta · Jignasa N. Solanki ·
Suresh Kumar Kailasa

Received: 14 February 2014 / Accepted: 11 May 2014 / Published online: 21 May 2014
© Springer-Verlag Wien 2014

Abstract We have developed a crown ether based selective colorimetric sensing scheme for the determination of Pb(II) ion by using gold nanoparticles modified with dithiocarbamate derivative of 4'-aminobenzo-18-crown-6 that acts as a colorimetric probe. Monodisperse Au-NPs were prepared by reacting 4'-aminobenzo-18-crown-6 with carbon disulfide to generate the dithiocarbamate ligand which was then added to the Au-NPs to form a supramolecular assembly on their surface. The Au-NPs modified in this way undergo aggregation in the presence of Pb(II) ions, and this causes the color to change from red to blue. The Pb(II)-induced aggregation can be monitored by using UV-visible spectrometry and even with the bare eye. The absorbance ratio ($A_{650\text{nm}}/A_{520\text{nm}}$) is linearly related to the concentration of Pb(II) in the 0.1 to 75 μM range (with a correlation coefficient of 0.9957), and the detection limit is 50 nM which is lower than the allowable level (75 nM) as defined by the US EPA. The method was successfully applied to the determination of Pb(II) in spiked water samples.

Keywords DTC-CE-Au NPs · Pb(II) ion · UV-visible spectrometry · FT-IR · TEM and DLS

Electronic supplementary material The online version of this article (doi:10.1007/s00604-014-1287-5) contains supplementary material, which is available to authorized users.

V. N. Mehta · S. K. Kailasa (✉)
Applied Chemistry Department, S. V. National Institute of
Technology, Surat 395 007, India
e-mail: sureshkumarchem@gmail.com

S. K. Kailasa
e-mail: skk@ashd.svnit.ac.in

J. N. Solanki
Chemical Engineering Department, S. V. National Institute of
Technology, Surat 395 007, India

Introduction

Lead contamination causes extensive environmental pollution and health problems in many parts of the world. Recent survey reveals that the human exposure to lead causes serious diseases in the nervous and cardiovascular systems [1]. It was noticed that the some areas in the world have been suffering from serious heavy metals contamination including lead at the cost of economy development and this has even directly influenced the supply of safe water for drinking and farming [2]. In this connection, the National Primary Drinking Water Regulations of USA has fixed the limit for the action level of lead ion in drinking water is 15 ng mL^{-1} [3]. Therefore, simple, fast and sensitive methods are essentially needed for monitoring water quality and for protecting human and animal health. As a result, a number of classical analytical techniques such as atomic absorption/emission spectrometry, inductively coupled plasma mass spectrometry, thermal ionization mass spectrometry, X-ray fluorescence spectrometry, anodic stripping voltammetry and cold vapor atomic fluorescence spectrometry have been extensively applied to detect heavy metal ions including lead in various samples with high sensitivity [4]. These approaches exhibit excellent performance at the expenses of expensive instrumentation, required time-consuming sample preparation and preconcentrations in which they involve tedious chemical processes for extracting metal ions. Importantly, these are incapable for on-site real time monitoring of lead in environmental samples. Therefore, a portable, low-cost, and fast analytical method is essentially needed for on-site/in-situ screening of Pb^{2+} ions-contaminated sites in environmental samples.

Recent years, much effort has been devoted to the design of metallic nanoparticles-based sensors for the detection of heavy metal ions in environmental samples. As for signal transducer, Au NPs are emerged as promising probes in colorimetric assays because of their high extinction coefficients

(10^8 – 10^{10} M⁻¹ cm⁻¹) in the visible region and distinct color change that attributes between their monodispersion and induced-aggregation states, which can be observed with bare eye [5]. The ultra-trace target metal ions were selectively identified by integrating functionalized Au NPs as colorimetric sensors in UV-visible spectrometry. For example, Su's group described the use of functionalized Au NPs with glutathione as optical probes for colorimetric assay of Pb²⁺ at 20 ppb level [6]. Similarly, Ray and co-workers developed a colorimetric method for detection of Pb²⁺ ion in plastic toys, paints and water samples by using glutathione conjugated Au NPs as nanosensors [7]. Liu's group developed a colorimetric method for the detection of Pb²⁺ ion based on the DNAzyme functionalized Au NPs induced agglomerations [8]. Other emerging approaches have developed for sensing of Pb²⁺ ion in water samples by using Au NPs capped with citrate [9], and cysteine-alanine-leucine-asparagine-asparagine (CALNN) [10] as probes. These sensing assays are based on the coordination chemistry between Pb²⁺ ion and functional groups on the surfaces of Au NPs. Recently, Kim et al. developed a novel solid-phase colorimetric method for the detection of Pb²⁺ ion at pM concentration by fabricating Au NPs into poly(oligo(ethylene glycol)methacrylate) [11].

Furthermore, significant progress has been made on the development of crown ethers (CE) based molecular assembly on metallic NPs for sensing of alkali and heavy metal ions. Since, CE derivatives are known as ionophores and exhibited inherent sensor selectivity towards various metal ions, which is due to their unique coordination chemistry with very specifically sized ions [12]. To support this assumption, Srivastava et al. studied the stability of Pb²⁺ and Cd²⁺ ions complexes with 15-crown-5, benzo-15-crown-5 and 18-crown-6, and dicyclohexano-18-crown-6 derivatives by using conductometric titrations [13]. As a result, CE-based supramolecular assembly have been designed on metallic NPs/QDs and used as sensors for alkali metal ions sensing. For example, Chou's group developed a novel fluorogenic sensor for the detection of K⁺ ion in aqueous media by using 15-crown-5 functionalized CdSe/ZnS QDs as fluorescent probes [14]. The same group synthesized 15-crown-5 functionalized Au NPs with the assistance of silica particles for sensing of K⁺ ion via sandwich complex [15]. Similarly, Menon and co-workers carried out the dithiocarbamate of *N*-benzyl-4-aminobenzo-15-crown-5 molecular assembly onto the surfaces of Au NPs and used as a colorimetric probe for selective sensing of K⁺ ion [16]. Chen's group developed a colorimetric method for selective binding of alkali metal ions (K⁺ and Na⁺) via "sandwich" complex model by using crown ether (15-crown-5)-modified Au NPs as a probe [17]. The same group described the use of 15-crown-5-CH₂O(CH₂)₁₂SH functionalized Au NPs for visual sensing of K⁺ ion, resulting a red-shift in their SPR peak [18]. In another work, Ramamurthy et al. described the use of aza-crown ether acridinedione functionalized Au

NPs as colorimetric and fluorometric chemosensors for sensing of Ca²⁺ and Mg²⁺ in aqueous solutions [19]. Inspired by these works, we decide to tune crown ether functionalized Au NPs that can serve as new alternative probe for sensing of other heavy metal ions instead of alkali metal ions. Since, tuning of Au NPs surfaces with active CE functional groups toward sensing and recognition of other metal ions is an important and as yet unexplored subject.

Herein, we report the tuning of Au NPs surfaces with DTC assemblies of 4'-aminobenzo-18-crown-6 and their exploitation as a visual sensing unit toward Pb²⁺ ion via sandwich complex between DTC-CE-Au NPs and Pb²⁺ ion (2:1) (Scheme 1). The present method was successfully applied to detect Pb²⁺ ion in water samples.

Experimental

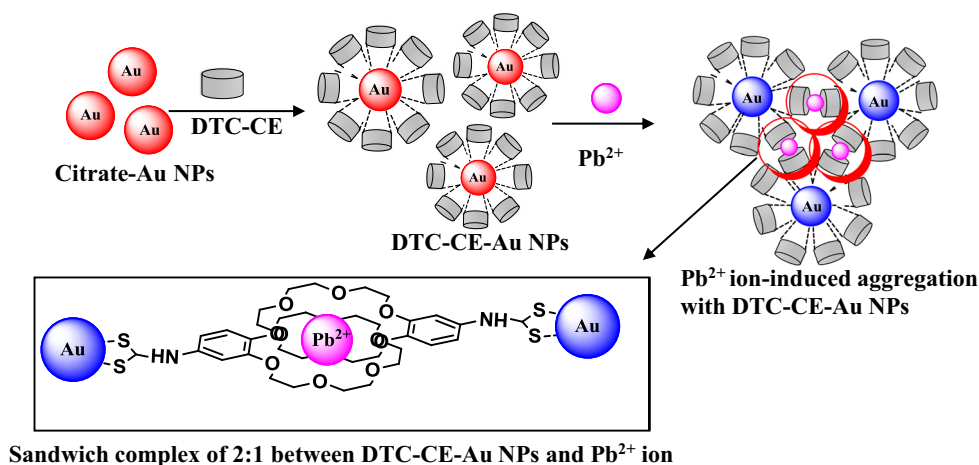
Chemicals and materials

Hydrogen tetrachloroaurate hydrate (HAuCl₄·xH₂O), 4'-aminobenzo-18-crown-6, 4-(2-hydroxyethyl)-1-piperazineethanesulfonic acid (HEPES), metal salts (Zn(NO₃)₂·6H₂O, Mn(NO₃)₂·4H₂O, Co(NO₃)₂·6H₂O, Pb(NO₃)₂, Cd(NO₃)₂·4H₂O, Cu(NO₃)₂·3H₂O, Hg(NO₃)₂·H₂O, FeCl₂·4H₂O, Mg(NO₃)₂·6H₂O, NiSO₄·6H₂O, FeCl₃·6H₂O, Cr(NO₃)₂·6H₂O, CaCl₂·2H₂O, AlCl₃, Na₂SO₄·10H₂O, KNO₃, Ba(NO₃)₂·4H₂O) were purchased from Sigma-Aldrich Corp. (USA, <http://www.sigmaaldrich.com>). Carbon disulfide and sodium chloride were obtained from Merck Ltd. (India, <http://www.merckmillipore.in/chemicals>) Trisodium citrate dihydrate was purchased from SD Fine Chemicals Ltd. (India, <http://www.sdfine.com>) All chemicals were of analytical grade and used without further purification. Milli-Q-purified water was used for the sample preparations. The pH value of HEPES buffer (10 mM) was adjusted by using 0.1 M NaOH or HCl. Milli-Q-purified water was used for the sample preparations.

Synthesis of DTC-CE-Au NPs

The Au NPs were prepared by the reduction of Au³⁺ ions with citrate [20]. The 4'-aminobenzo-18-crown-6 (1.6 mg, 1.0 mM) was dissolved in 5 mL of absolute EtOH and then treated with CS₂ (5 mL, 1 mM). The reaction mixture was sonicated for 20 min to generate the dithiocarbamate ligand. For the preparation of DTC-CE-Au NPs, 250 μL of DTC-CE was added into a reaction flask that contained 20 mL of citrate capped Au NPs and the reaction mixture was stirred for 1 h to ensure supramolecular assembly of DTC-CE ligands on Au NPs surfaces (Supporting Information of Fig. S1). The DTC-CE-Au NPs were stable in aqueous solution at 4 °C for several

Scheme 1 Schematic representation of Pb²⁺ ion-induced DTC-CE-Au NPs aggregation via sandwich complex formation



days. The size and morphology of DTC-CE-Au NPs were characterized by DLS and TEM.

Visual sensing of Pb²⁺ ion with DTC-CE-Au NPs

In order to investigate visual sensing ability of DTC-CE-Au NPs towards metal ions, various metal ions such as alkali (Na⁺ and K⁺), alkaline earth (Mg²⁺, Ca²⁺ and Ba²⁺), and heavy and transition metal ions (Cd²⁺, Cu²⁺, Co²⁺, Mn²⁺, Ni²⁺, Hg²⁺, Fe²⁺, Zn²⁺, Cr³⁺, Al³⁺, Fe³⁺ and Pb²⁺) were added independently into 1.0 mL of DTC-CE-Au NPs solution at HEPES buffer pH 7.0. The sample vials were vortexed for 30 s and the color of the solutions were recorded by using digital camera. The SPR peak changes of DTC-CE-Au NPs were measured by UV-visible spectrometry.

Determination of Pb²⁺ in water samples

The DTC-CE-Au NPs were used as probes for sensing of Pb²⁺ ion in water samples (drinking water, tap water and river water). The drinking water and tap water were collected from the research laboratory of SVNIT, Surat. River water was taken from the Tapi River, Surat. The collected samples were filtered through 0.45 μm membrane, spiked with the different concentration of Pb²⁺ ion (10, 50 and 100 μM) and then analyzed by the aforesaid procedure.

Instrumentation

UV-vis absorption spectra were recorded by using a Maya Pro 2,000 spectrophotometer (Ocean Optics, USA, <http://www.oceanoptics.com>) at room temperature. ¹H NMR spectra were recorded on a Varian 400 MHz instrument (USA, <http://www.agilent.com>). Fourier transform infrared (FT-IR) spectra were recorded on a Perkin Elmer (FT-IR spectrum BX, Germany, <http://www.perkinelmer.com>). Transmission electron microscopy (TEM) images were

taken on a Tecnai 20 (Philips, Holland, <http://www.innovationservices.philips.com>) at an acceleration voltage of 100 kV. DLS measurements were performed by using Zetasizer Nano ZS90 (Malvern, UK, <http://www.malvern.com>). Energy dispersive X-ray spectra (EDS) were recorded by using JSM-7,600 F (Jeol, Japan, <http://www.jeol.co.jp>).

Results and discussion

Characterization of DTC-CE-Au NPs

Before the characterization of DTC-CE-Au NPs, we studied the effect of the concentration (1.0 mM, 125–1,000 μL) of DTC-CE ligands on Au NPs. As shown in Supporting Information of Fig. S2, the characteristic SPR peak of Au NPs was gradually changed with increasing concentration of DTC-CE ligands on Au NPs, resulting color change from red to blue. To control the color of Au NPs and to maintain SPR peak at ~520 nm, we selected 250 μL of 1.0 mM DTC-CE as the best optimum concentration for its effective molecular assembly onto the surfaces of Au NPs. The structural confirmations of DTC-CE and DTC-CE-Au NPs were carried by using spectroscopic (UV-visible, FT-IR, ¹H NMR) techniques. The size and morphology of DTC-CE-Au NPs were investigated by using DLS and TEM. As shown in Supporting Information of Fig. S3, the UV-visible absorption spectrum of citrate capped Au NPs exhibits the characteristic SPR peak of Au NPs at 517 nm, however, a very slight red-shift was attributed after functionalization of Au NPs with DTC-CE molecules, in which the SPR peak was shifted to 520 nm (red line). This is due to certain induce SPR interactions on the surfaces of Au NPs via a simple “zero-length” covalent coupling of -SH groups of DTC-CE, which yields a slight bathochromic shift of SPR band from 517 nm (citrate capped Au NPs) to 520 nm for DTC-CE-Au NPs.

Supporting Information of Fig. S4 shows the typical FT-IR spectra of 4'-aminobenzo-18-crown-6, DTC-CE and DTC-CE-Au NPs, respectively. The peaks at 954, 1,184, 1,284 and 1,456 cm^{-1} correspond to the stretching and vibration modes of crown moiety. The peaks at 900–670 cm^{-1} are assigned to the aromatic stretching bands of =C–H in CE. The peaks at 1,641 and 1,491 cm^{-1} correspond to the in-plane vibrations of aromatic –C=C– in CE. The peaks at 2,849 and 2,915 cm^{-1} are corresponded to the $\nu_a(\text{CH}_2)$ and $\nu_{as}(\text{CH}_2)$ bands in CE. It can also be observed that the FT-IR spectrum of DTC-CE exhibits new peaks at 2,541, 1,051, and 1,275 cm^{-1} , which are corresponded to –SH, C–S, and CS–NH stretching and bending vibrations in DTC-CE (Supporting Information of Fig. S4b). Importantly, the mercapto group stretching and bending vibrations of DTC-CE molecules were disappeared at 2,541 cm^{-1} in DTC-CE-Au NPs, which confirms that the formation of covalent bond between –SH group of DTC-CE and the surfaces of Au NPs (Supporting Information of Fig. S4c).

Supporting Information of Fig. S5 shows the ^1H NMR spectra of pure 4'-aminobenzo-18-crown-6, DTC-CE and DTC-CE-Au NPs. The ^1H NMR spectrum of pure CE exhibits peaks at 6.82–7.50 and at 9.11 δ ppm corresponded to the protons of aromatic and –NH₂ groups in 4'-aminobenzo-18-crown-6. The peaks between 3.60–3.91 δ ppm attributed to methylene protons of CE. Importantly, it can be noticed that the new peak at 1.16 δ ppm was assigned to –SH group of DTC-CE (Supporting Information of Fig. S5b). However, ^1H NMR spectrum of DTC-CE-Au NPs did not exhibit any proton peaks, which represents the up-field chemical shift of all the protons in DTC-CE-Au NPs.

The dispersability and hydrodynamic diameter of citrate capped Au NPs and DTC-CE-Au NPs were measured by using DLS. As shown in Fig. 1a–b, the citrate capped Au NPs are in monodisperse with an average hydrodynamic diameter of 5 nm. However, the hydrodynamic diameter of DTC-CE-Au NPs was slightly increased to 43 nm, which is due to the DTC-CE molecular assembly on Au NPs surfaces. Figure 2a shows the TEM image of DTC-CE-Au NPs and the average particle size was \sim 50 nm, suggesting that the DTC-CE-Au NPs are well dispersed with spherical shape in the solution. Supporting Information of Fig. S6a–b shows the EDS spectra of citrate capped Au NPs and DTC-CE-Au NPs. It can be observed that the sharp optical absorption peak in the range of 2 to 12 keV is attributed to the absorption of metallic Au NPs. The C, O, S, and Na signals were attributed from DTC-CE-Au NPs.

Ionic radius-based selective visual sensing of Pb^{2+} ion

In order to establish DTC-CE-Au NPs as metal ion selective sensor, we investigated UV–visible spectra of DTC-CE-Au NPs after additions of various metal ions (alkali metal ions - Na^+ , K^+ ; alkali earth metal ions - Mg^{2+} , Ca^{2+} and Ba^{2+} ; transition and

heavy metal ions - Cd^{2+} , Cu^{2+} , Co^{2+} , Mn^{2+} , Ni^{2+} , Hg^{2+} , Fe^{2+} , Zn^{2+} , Cr^{3+} , Al^{3+} , Fe^{3+} and Pb^{2+} , 1.0 mM) at HEPES buffer pH 7.0. As shown in Fig. 3a, the characteristic SPR peak intensity of DTC-CE-Au NPs at 520 nm was drastically decreased with appearing a new SPR peak at 650 nm by only the addition of Pb^{2+} ion, resulting in a color change from red to blue, which can be visualized with bare eye (Fig. 3b). These results revealed that the other metal ions such as alkali metal ions (Na^+ , K^+), alkali earth metal ions (Mg^{2+} , Ca^{2+} , Ba^{2+}), transition/heavy metal ions (Cd^{2+} , Cu^{2+} , Co^{2+} , Mn^{2+} , Ni^{2+} , Hg^{2+} , Fe^{2+} , Zn^{2+} , Cr^{3+} , Al^{3+} , Fe^{3+}) did not show any obvious effect on the SPR peak and color of DTC-CE-Au NPs as compared to Pb^{2+} ion, confirming that only Pb^{2+} ion induces the aggregation of DTC-CE-Au NPs, which yielded a red-shift in their UV-visible spectrum. Supporting Information of Fig. S7 shows the colorimetric sensing ability of DTC-CE-Au NPs in terms of absorbance ratio at 650 nm to that at 520 nm ($A_{650\text{nm}}/A_{520\text{nm}}$), indicating that DTC-CE-Au NPs showed high selectivity towards Pb^{2+} than the other metal species. Furthermore, we studied the effect of DTC-CE concentration (1.0 mM, 125–1,000 μL) on Au NPs for effective colorimetric sensing of Pb^{2+} ion. Supporting Information of Fig. S8 shows the UV-visible spectra and photograph of Au NPs in presence of Pb^{2+} (1.0 mM) at different concentration of DTC-CE (1.0 mM, 125 to 1,000 μL). These results demonstrated that the maximum absorption ratio ($A_{650\text{nm}}/A_{520\text{nm}}$) was observed only at 250 μL of 1.0 mM DTC-CE-Au NPs in the presence of Pb^{2+} , indicating that 250 μL of 1.0 mM DTC-CE is more suitable for the effective Pb^{2+} ion-induced aggregation of DTC-CE-Au NPs. Therefore, we selected 250 μL of 1.0 mM DTC-CE as the best concentration for capping of Au NPs to visualization of Pb^{2+} ion.

Effect of pH

The stability of DTC-CE-Au NPs was investigated at different pH values without addition of Pb^{2+} . As shown in Fig. 4a, the UV-visible absorption spectra of DTC-CE-Au NPs were red-shifted towards longer wavelengths (640 nm) in pH range from 2.0 to 4.0, yielding a color change from red to blue, which confirms that self-aggregation of DTC-CE-Au NPs through surface charge neutralization. It can be noticed that the UV-visible absorption spectra and color of DTC-CE-Au NPs are remained unchanged at pH range from 5.0 to 12, which indicates that DTC-CE-Au NPs are dispersed in the solution. Furthermore, we also examined the effect of HEPES buffer pH ranging from 2.0 to 12 for effective aggregation of DTC-CE-Au NPs induced by Pb^{2+} ion (Fig. 4b). As shown in Fig. 4b, the UV-visible spectra of DTC-CE-Au NPs with Pb^{2+} at HEPES buffer pH range of 8.0 to 12 have shown exactly SPR peak at 520 nm, just as we observed in DTC-CE-Au NPs spectrum. These results indicate that the Pb^{2+} ion-induced DTC-CE-Au NPs aggregation did not occur in this pH. It can also be observed that the absorption spectra of DTC-CE-

Fig. 1 DLS of (a) citrate capped Au NPs (b) DTC-CE-Au NPs and (c) Pb²⁺ ion-induced DTC-CE-Au NPs aggregation

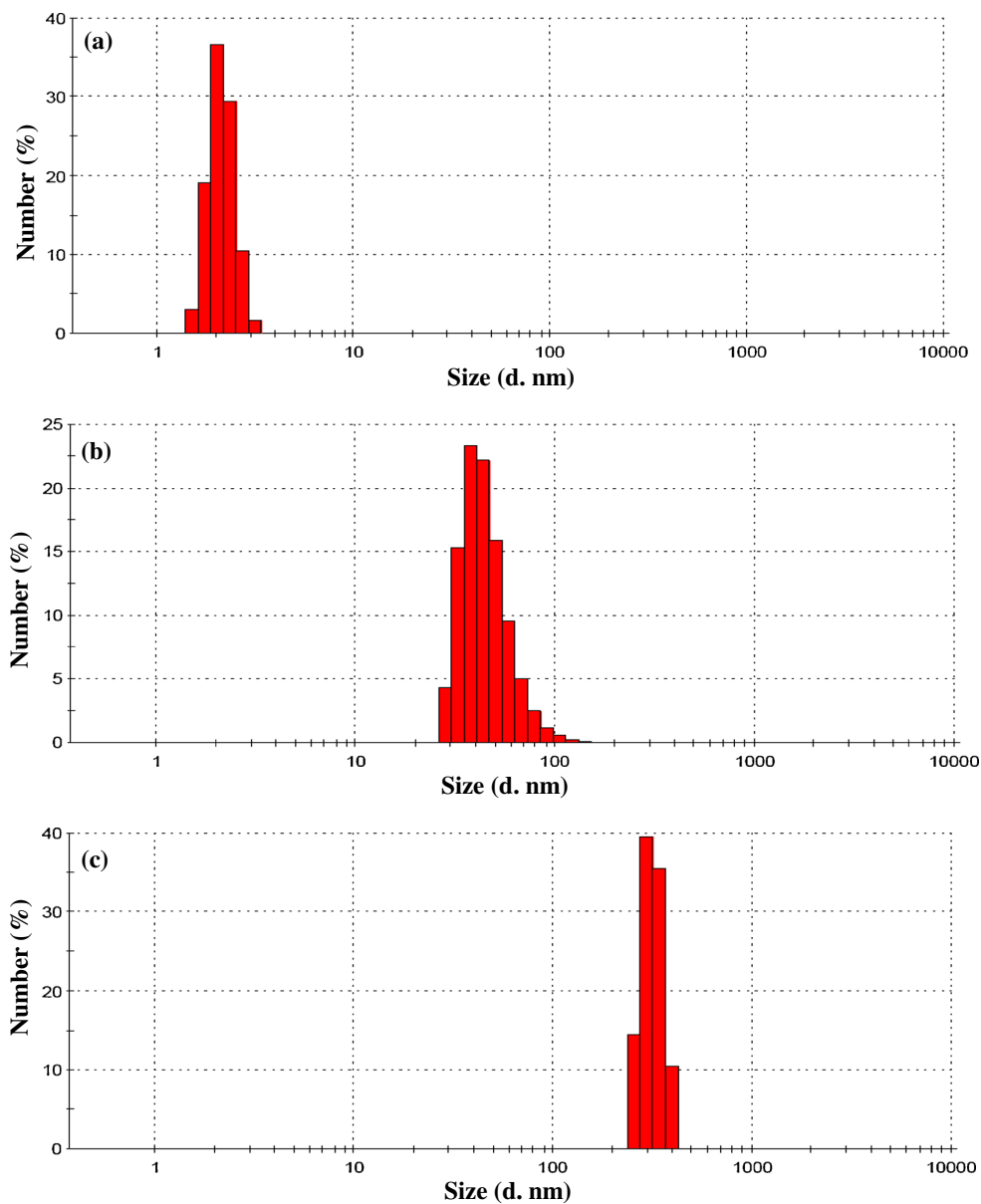


Fig. 2 TEM images of (a) DTC-CE-Au NPs and (b) Pb²⁺ ion-induced DTC-CE-Au NPs aggregation

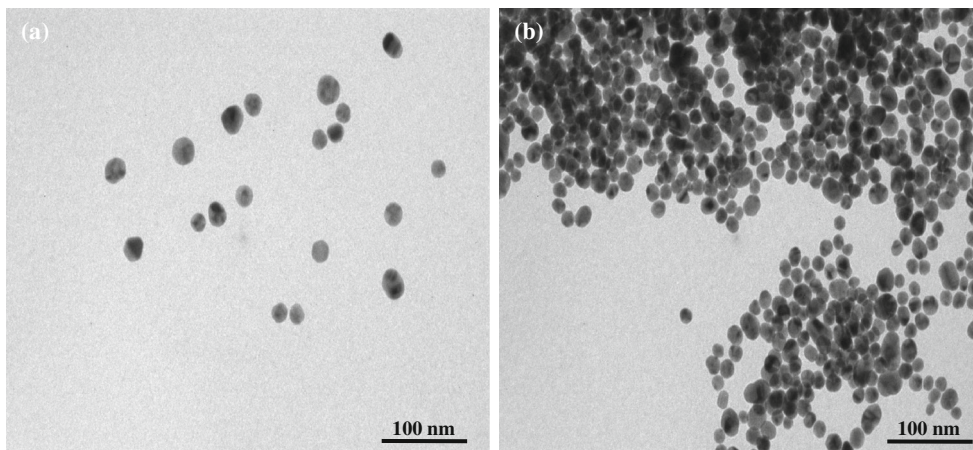
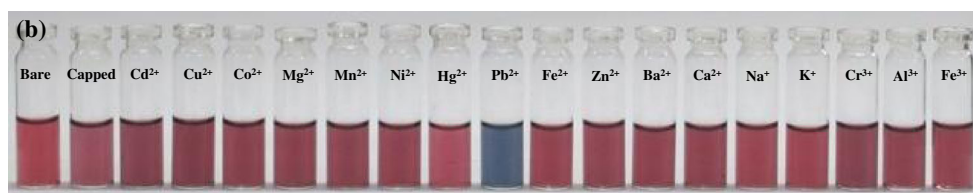
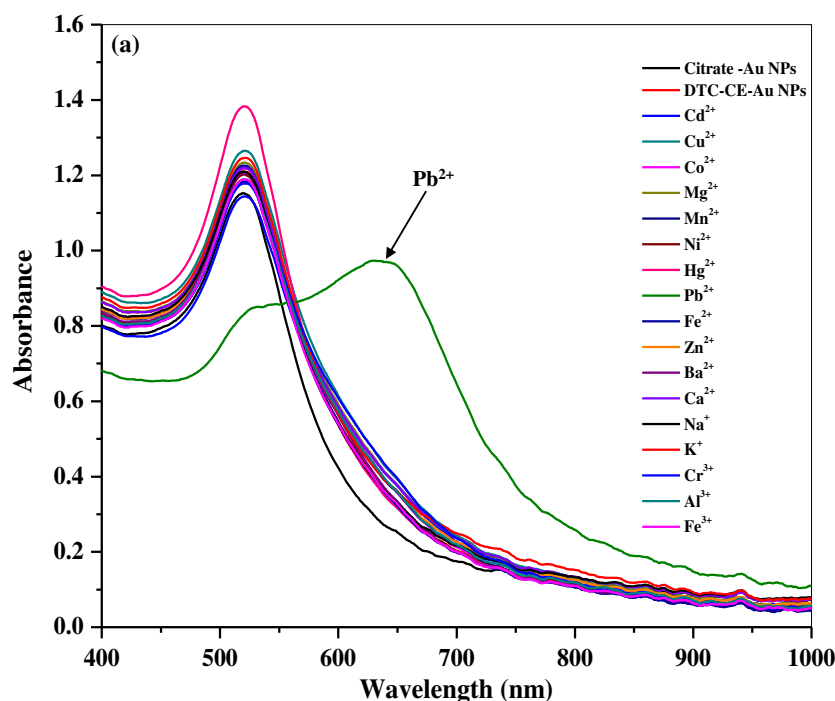


Fig. 3 The relative absorption ratio ($A_{650\text{ nm}}/A_{520\text{ nm}}$) of Pb^{2+} ion-induced DTC-CE-Au NPs aggregation over other metal ions (alkali metals - Na^+ , K^+ ; alkali earth metal ions - Mg^{2+} , Ca^{2+} , Ba^{2+} and transition/heavy metal ions - Cd^{2+} , Cu^{2+} , Co^{2+} , Mn^{2+} , Ni^{2+} , Hg^{2+} , Fe^{2+} , Zn^{2+} , Cr^{3+} , Al^{3+} , Fe^{3+} and Pb^{2+}) at HEPES buffer pH 7.0. **b** photographic image of DTC-CE-Au NPs in the presence of various metal ions (Na^+ , K^+ , Mg^{2+} , Ca^{2+} , Ba^{2+} , Cd^{2+} , Cu^{2+} , Co^{2+} , Mn^{2+} , Ni^{2+} , Hg^{2+} , Fe^{2+} , Zn^{2+} , Cr^{3+} , Al^{3+} , Fe^{3+} and Pb^{2+})



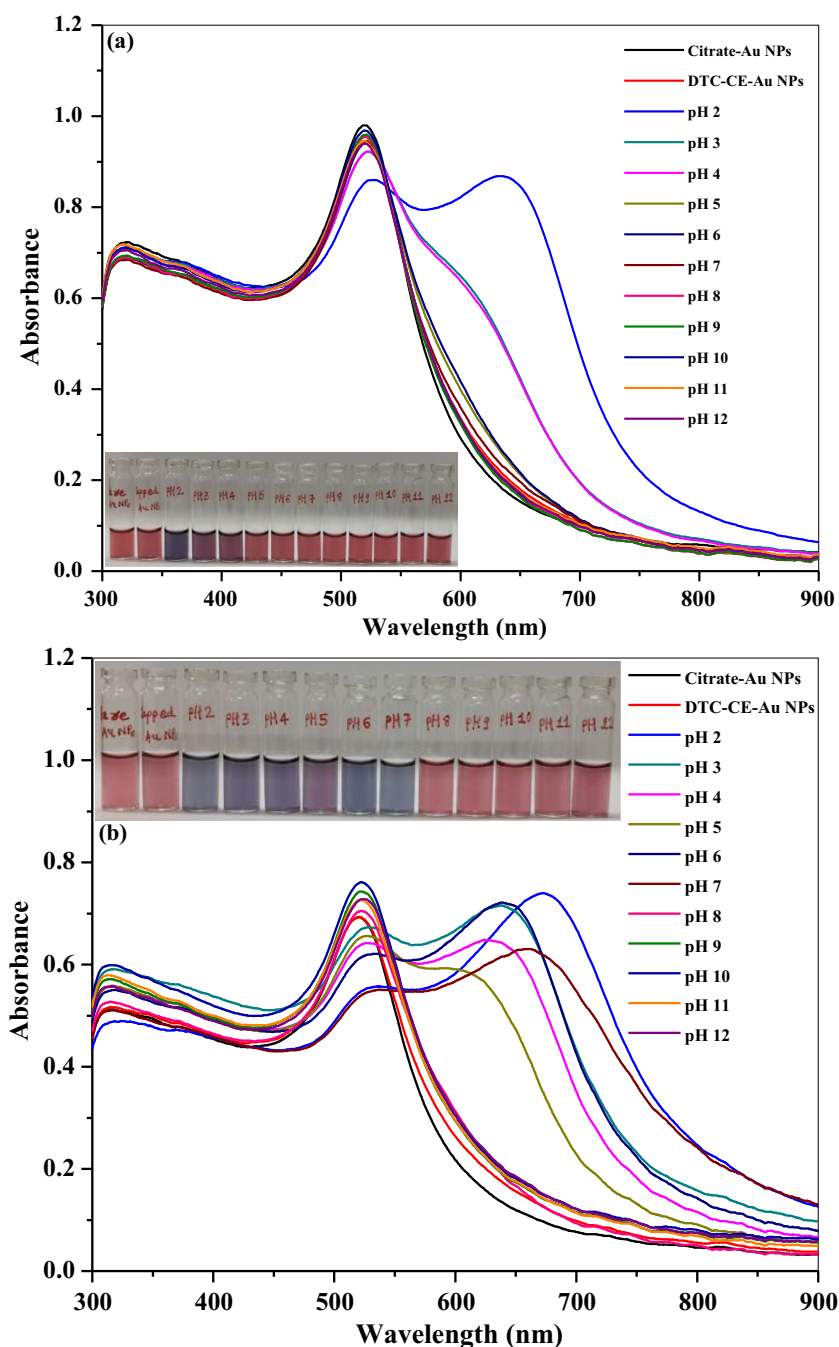
Au NPs with Pb^{2+} ion at HEPES buffer pH from 2.0 to 4.0 were drastically changed with the generation of new SPR peak at 680 nm, which confirms that the surface charges neutralizations of Au NPs at acidic pH ($\text{pH} < 5.0$). Importantly, this peak is not attributed from Pb^{2+} ion-induced aggregation of DTC-CE-Au NPs. Moreover, the oxygen atom in the crown ether moiety gets protonated in the acidic conditions and hydrolysis of Pb^{2+} takes place at higher pH values ($\text{pH} > 8$) which resist to form the sandwich complex of 2:1 between DTC-CE-Au NPs and Pb^{2+} . Importantly, it can be observed that the intensity of characteristic SPR peak of DTC-CE-Au NPs was drastically decreased and a new SPR peak was generated at 650 nm, confirming strong DTC-CE-Au NPs aggregation induced by Pb^{2+} through sandwich complex of 2:1 between DTC-CE-Au NPs and Pb^{2+} ion at HEPES buffer pH 7.0. Therefore, we selected HEPES buffer pH 7.0 as optimum pH for effective aggregation of DTC-CE-Au NPs induced by Pb^{2+} ion.

Sensing mechanism

It is well known that crown ethers are used as the molecular scavenger and exhibited an outstanding ability to selectively

coordinate with the metal ions based on their ionic radius [21, 22]. They also acted as selective binding agents for organic molecules through the host-guest complexation between CE and organic molecules [23]. Importantly, CE molecules contain hetero atoms in the centre of a crown ether molecule, which can act as electron donor to various metal ions. The complexing ability of CE always depends on the sizes of CE cavity and metal ions, since the sizes of hosts (CE) pockets or cavities should be suited with the guest molecule size. To support this assumption, several crown ethers cavities 15-Crown-5 - Na^+ [17], 15-Crown-5 - K^+ [14, 15], 15-crown-5- and 15-crown-4- Na^+ and K^+ [18], 1-aza-15-crown-5- Ca^{2+} and Mg^{2+} [19], and DTC-benzo-15-crown-5 - K^+ [16] have described the role of cavity size towards metal ions. These reports indicate that the crown ethers have exhibited partially pre-organized configuration, and showed high complex formation ability towards cations [24]. As a result, sandwich complex between the crown ether moieties and alkali/alkaline earth metal ions is possible. These sandwich complexations are attributed by using crown ether moieties sizes from 15-crown-4- to 15-crown-5-, which are well fit for alkali/alkali earth metal ions [24]. To alter their affinity towards other metal ions, we design large crown ether (DTC

Fig. 4 UV-visible absorption spectra and photographs of (a) DTC-CE-Au NPs in the pH range of 2–12 and (b) presence of Pb²⁺ ion in the pH range of 2–12



4'-aminobenzo-18-crown-6) moiety on Au NPs surfaces to interact with other metal ions instead of alkali/alkali earth metal ions. As shown in Fig. 3b, the designed DTC-CE-Au NPs showed high affinity towards Pb²⁺ ion, resulting color change from red to blue. The obtained results are quite different from the literature in which they used 15-crown-4- and 15-crown-5- functionalized Au NPs for either alkali or alkali earth metal ions [14–19].

To support this hypothesis, Pedersen and Jackson studied the complexation ability based on the sizes of 18-crown-6- and 15-crown-6- and ionic radius of lead ions (II and IV) [25,

26]. It has been observed that the Pb²⁺ ion showed high affinity to interact with 18-crown-6 instead of 15-crown-6. This reason is due to the diameter of Pb²⁺ ion (2.4 Å) could effectively fit into the cavity size of 18-crown-6 (2.2–3.2 Å). Since, the cavity size of 15-crown-6 in between 1.7 and 2.2 Å, which is not suitable to fit Pb²⁺ ion in the 15-crown-6 cavity [25]. It was also observed that the Pb⁴⁺ ion has extremely smaller ion-dipole interactions with crown cavity, since the diameter of Pb⁴⁺ ion is 0.84 Å, which inhibits its complex formation with crown ether [26]. Based on these hypothetical explanations, we believe that the size of crown

ether cavity plays an important role to fit Pb^{2+} ion diameter exactly into the cavity of 18-crown-6 through sandwich complex of 2:1 between 18-crown-6 moiety and Pb^{2+} ion, resulting in the red shift of SPR peak due to Pb^{2+} ion-induced DTC-CE-Au NPs aggregation (Fig. 3a). To confirm Pb^{2+} ion-induced DTC-CE-Au NPs aggregations, we studied DLS and TEM of the DTC-CE-Au NPs. It can be observed that the hydrodynamic diameter of DTC-CE-Au NPs was greatly increased to 396 nm, which confirms that their change from monodisperse to polydisperse upon the addition of Pb^{2+} ion (Fig. 1c). The obtained TEM image of DTC-CE-Au NPs exhibits well aggregation between DTC-CE-Au NPs, which confirms that the formation of sandwich complex of 2:1 between DTC-CE-Au NPs and Pb^{2+} ion (Fig. 2b). As shown in Supporting Information of Fig. S6c, the EDS spectrum of Pb^{2+} ion-induced DTC-CE-Au NPs aggregation exhibited the sharp optical absorption peaks in the range of 2 to 6 keV, which are corresponded to Pb, Au, C, O, S, and Na signals of Pb^{2+} ion-induced DTC-CE-Au NPs aggregation. In order to explain the role of DTC-CE on Au NPs for colorimetric sensing of Pb^{2+} ion, the control experiments were performed by using the citrate capped Au NPs and DTC-CE-Au NPs as probes for colorimetric sensing of Pb^{2+} ion. As shown in Supporting Information of Fig. S9, there is no change in the

UV-visible spectrum and color of citrate capped Au NPs in the presence of Pb^{2+} , which indicates of the aggregation of citrate capped Au NPs is not induced by Pb^{2+} . However, the aggregation of DTC-CE-Au NPs was induced by Pb^{2+} , which results a red-shift in their absorption spectra from 520 to 650 nm and a color change from red to blue. Based on these result, we confirmed that DTC-CE molecular assembly on Au NPs play key role for the aggregation of DTC-CE-Au NPs induced by Pb^{2+} via formation of sandwich complex of 2:1 between DTC-CE-Au NPs and Pb^{2+} ion.

Effect of NaCl concentration

It is well known that the sensitivity and dynamic range of NPs-based UV-visible spectrometric method is dependent on the resistance of NPs to aggregate and this can be optimized by changing the Au NPs buffer composition [27]. To support this, Lin's group studied the effective metal ion-induced NPs aggregations by using NaCl as ionic strength [28]. To enhance the sensitivity of probe, we studied the effect of UV-visible spectra of DTC-CE-Au NPs by the addition of NaCl ranging from 0.005 to 0.040 M (Supporting Information of Fig. S10). As shown in Supporting Information of Fig. S10, the color

Fig. 5 **a** UV-visible spectra of DTC-CE-Au NPs solutions with various concentrations of Pb^{2+} in the range of 0.1 to 1,000 μM . **b** Color change of DTC-CE-Au NPs with the addition of different concentrations of Pb^{2+} ranging from 0.1 to 1,000 μM

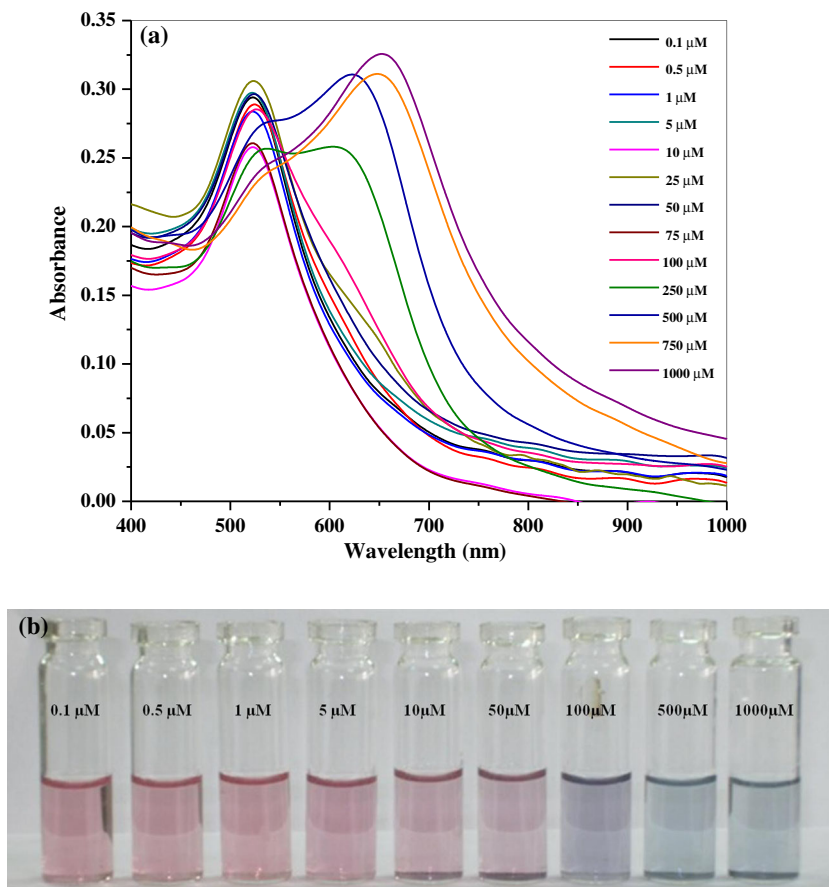
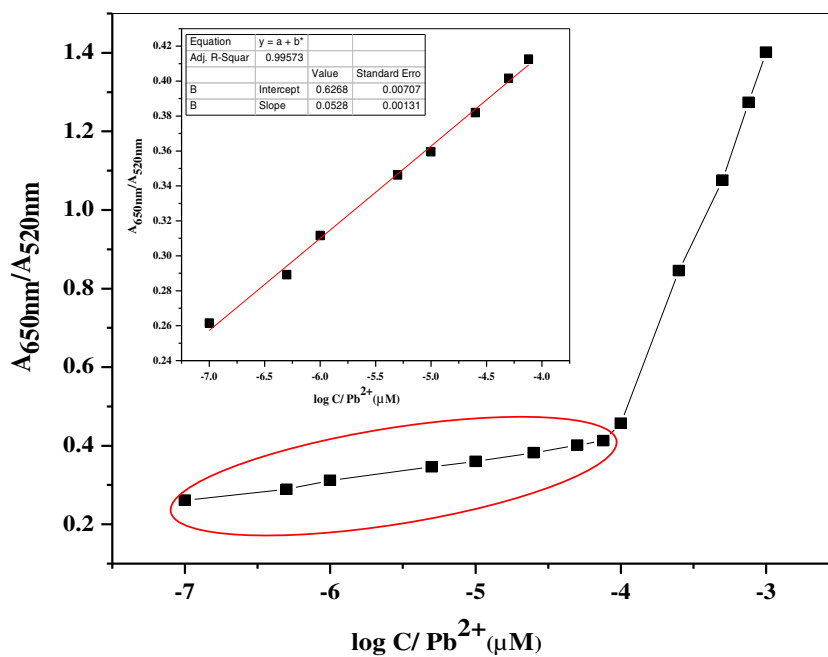


Fig. 6 Calibration graph between the absorption ratio at $A_{650\text{ nm}}/A_{520\text{ nm}}$ and concentration of Pb^{2+} by using DTC-CE-Au NPs as a colorimetric probe



and SPR peak of DTC-CE-Au NPs did not change up to the addition of NaCl concentration from 0.005 to 0.020 M. However, the color and UV-visible spectra of DTC-CE-Au NPs are changed by the addition of excess NaCl ranging from 0.025 to 0.040 M, resulting Au NPs aggregations due to excess NaCl which leads to decrease in electrostatic repulsion between Au NPs. Supporting Information of Fig. S11 shows the absorbance ratio ($A_{650\text{ nm}}/A_{520\text{ nm}}$) of DTC-CE-Au NPs before and after addition of 1.0 mM Pb^{2+} in presence of different concentrations of NaCl. It can be noticed that the absorbance ratio ($A_{650\text{ nm}}/A_{520\text{ nm}}$) is increasing with increasing concentration of NaCl. These results indicate that the sensing ability of DTC-CE-Au NPs is greatly improved by the addition of 0.020 M NaCl. To confirm this, we also studied the UV-visible absorption spectra of DTC-CE-Au NPs by the addition of Pb^{2+} ion without NaCl (Supporting Information of Fig. S12). We observed that the absorption ratio ($A_{650\text{ nm}}/$

$A_{520\text{ nm}}$) was greatly improved by the addition of lower concentrations of Pb^{2+} in the presence of NaCl. Therefore, we carried out the analysis of Pb^{2+} ion by using DTC-CE-Au NPs in the presence of 0.020 M NaCl.

Linear range

In order to evaluate the sensitivity of the method, different concentrations of Pb^{2+} ion were added into the DTC-CE-Au NPs solution that contained 0.020 M of NaCl by using HEPES buffer at pH 7.0. As shown in Fig. 5, we noticed that the color of the solutions was gradually changed from red to blue upon increasing concentration of Pb^{2+} ion from 0.1 to 1,000 μM , which confirms the greater degree of Pb^{2+} ion-induced DTC-CE-Au NPs aggregation. Moreover, the SPR peak intensity of DTC-CE-Au NPs at 520 nm decreased with increasing concentration of Pb^{2+} ion, resulting in the increase

Table 1 Comparison of DTC-CE-Au NPs as colorimetric probe for the determination of Pb^{2+} with the reported methods

NPs	Capping agent	Size (nm)	LOD (M)	Technique	References
Au NPs	Glutathione	5–8	100×10^{-9}	UV-visible	[6]
Au NPs	Glutathione	–	100 ppt	DLS	[7]
Au NPs	ssDNA	6.1	6.2×10^{-12}	DLS	[29]
Au NPs	Gallic acid	12.0	10^{-9}	UV-visible	[30]
Au NPs	Sodium thiosulfate hexadecyl Trimethyl ammonium bromide	12.6	40×10^{-9}	UV-visible	[31]
Au NPs	Papain	13	200×10^{-9}	UV-visible	[32]
Ag NPs	Diethanolamine dithiocarbamate	28.6	4×10^{-9}	RLS	[33]
Ag NPs	Iminodiacetic acid	7–10	13×10^{-9}	UV-visible	[34]
Ag NPs	Aza-crown-ether	10	2.5×10^{-11}	DLS	[35]
Au NPs	DTC-CE-Au NPs	10	50×10^{-9}	UV-visible	Present study

of new SPR peak intensity at 650 nm (Fig. 5a). Using this, a calibration curve was plotted between absorption ratio ($A_{650\text{nm}}/A_{520\text{nm}}$) and the logarithm of Pb^{2+} ion concentration over the range of 0.1 to 75 μM (Fig. 6). This probe exhibited a good correlation ($R^2=0.9957$), and the limit of detection (LOD) is 50 nM, which is calculated by multiplying the standard deviation of the blanks by three. Table 1 shows the comparison of present method for the detection of Pb^{2+} ion with the reported methods by using NPs-assisted DLS, Resonance light scattering (RLS) and UV-visible methods. The LOD obtained in this study is in good agreement with those reported metallic (Au and Ag) NPs-assisted UV-visible [6, 30–32, 34], DLS [7, 29, 35] and RLS [33] methods in the literature and exhibited superior LOD than the reported methods [6, 7, 29–35], suggesting that this approach is suitable for routine Pb^{2+} ion assays in environmental matrices. It was observed that the sensitivity of this probe to Pb^{2+} is not comparable with that of ssDNA-capped Au NPs [29] and aza-crown-ether capped Ag NPs [35] because of more number of anchoring groups on the surfaces of Ag NPs [29, 35]. However, this probe was successfully applied for selective and sensitive detection of Pb^{2+} ion in environmental samples.

Interference studies

In order to explore the potentiality of DTC-CE-Au NPs probe for Pb^{2+} ion, we studied the UV-visible spectrum of DTC-CE-Au NPs with Pb^{2+} ion (500 μM) in the presence of Na^+ , K^+ , Mg^{2+} , Ca^{2+} , Ba^{2+} , Cd^{2+} , Cu^{2+} , Co^{2+} , Mn^{2+} , Ni^{2+} , Hg^{2+} , Fe^{2+} , Zn^{2+} , Cr^{3+} , Al^{3+} and Fe^{3+} at 1.0 mM. As shown in Supporting Information of Fig. S13, the absorption spectra did not show any change in the presence of different metal ions, which confirms that the other metal ions are not interfered with the Pb^{2+} ion-induced DTC-CE-Au NPs aggregation. This result revealed that the DTC-CE-Au NPs can be effectively used as probe for the detection of Pb^{2+} ion in biological and environmental samples with high salinity.

Application of DTC-CE-Au NPs for the analysis of water samples

To evaluate the feasibility of DTC-CE-Au NPs for sensing of Pb^{2+} ion in water samples, we spiked different concentrations of Pb^{2+} ion in water samples (drinking, tap and river water) and the concentration of Pb^{2+} ion was estimated by the afore-said procedure. As shown in Supporting Information of Table S1, this method shows good recoveries from 97.6 to 102.1 %, with relative standard deviation 0.696 to 1.584 %. These results indicate that the present method exhibited great potentiality for the analysis of Pb^{2+} ion in real samples with good accuracy and precision.

Conclusions

In conclusion, the DTC-CE-Au NPs acted as a novel ionic-radius based colorimetric probe for selective sensing of Pb^{2+} ion. The effective Pb^{2+} ion-induced DTC-CE-Au NPs aggregation was achieved by the sandwich complex formation between multiple DTC of 4'-aminobenzo-18-crown-6-capped Au NPs and Pb^{2+} ion, yielding a red-shift in SPR peak of DTC-CE-Au NPs. The Au NPs aggregation was achieved by the matching of 4'-aminobenzo-18-crown-6- cavity size with the ionic radius of Pb^{2+} ion. As a result, this method showed good linearity in the range of 0.1 to 75 μM with a detection limit of 50 nM. The DTC-CE-Au NPs probe provides a simple analytical tool for determination of Pb^{2+} ion with good selectivity and sensitivity. Therefore, this ionic-radius-based DTC-CE-Au NPs sensor can be suitable for selective sensing of Pb^{2+} ion complex samples with minimized sample preparations.

Acknowledgment We thank the Director, SVNIT for providing all the facilities to carry out this work. We also thank Department of Science and Technology, India for providing UV-visible spectrophotometer under Fast-track Young Scientist Program (SR/FT/CS-54/2010). We would like to thank Mr. Vikas Patel, SICART, V. V. Nagar, Anand for their assistance in TEM data. We thank Prof. Z.V.P. Murthy and Mr. Chetan Patel, Chemical Engineering Department, SVNIT, Surat, India for providing DLS measurements.

References

1. Global health risks: Mortality and burden of disease attributable to selected major risks. Geneva, World Health Organization, 2009 (http://www.who.int/healthinfo/global_burden_disease/GlobalHealthRisks_report_full.pdf, accessed 20 December 2010)
2. Exposure to lead: A major public health concern. Geneva, World Health Organization, 2010 (<http://www.who.int/ipcs/features/lead.pdf>, accessed 20 December 2010).
3. <http://water.epa.gov/drink/contaminants/>
4. Casas JS, Sordo J (2006) Lead: chemistry, analytical aspects, environmental impact and health effects. Elsevier, Amsterdam
5. Lin YW, Huang CC, Chang HT (2011) Gold nanoparticle probes for the detection of mercury, lead and copper ions. *Analyst* 136:863–871
6. Chai F, Wang C, Wang T, Li L, Su Z (2010) Colorimetric detection of Pb^{2+} using glutathione functionalized gold nanoparticles. *ACS Appl Mater Interfaces* 2:1466–1470
7. Beqa L, Singh AK, Khan SA, Senapati D, Arumugam SR, Ray PC (2011) Gold nanoparticle-based simple colorimetric and ultrasensitive dynamic light scattering assay for the selective detection of Pb(II) from paints, plastics, and water samples. *ACS Appl Mater Interfaces* 3:668–673
8. Liu J, Lu Y (2004) Accelerated color change of gold nanoparticles assembled by DNazymes for simple and fast colorimetric Pb^{2+} detection. *J Am Chem Soc* 126:12298–12305
9. Guan J, Jiang L, Zhao LL, Li J, Yang WS (2008) pH-dependent response of citrate capped Au nanoparticle to Pb^{2+} ion. *Colloid Surf A* 325:194–197

10. Wei H, Li BL, Li J, Dong SJ, Wang EK (2008) DNAzyme-based colorimetric sensing of lead (Pb^{2+}) using unmodified gold nanoparticle probes. *Nanotechnology* 19:95501
11. Ferhan AR, Guo L, Zhou X, Chen P, Hong S, Kim DH (2013) Solid-phase colorimetric sensor based on gold nanoparticle-loaded polymer brushes: lead detection as a case study. *Anal Chem* 85:4094–4099
12. Gokel GW, Leevy WM, Michelle EW (2004) Crown ethers: sensors for ions and molecular scaffolds for materials and biological models. *Chem Rev* 104:2723–2750
13. Ijeri VS, Srivastava AK (2002) Complexation of macrocyclic compounds with metal ions: 1. Cd(II), Pb(II), Co(II), Mn(II), and Ag(I) ions in 40 vol ethanol + water medium. *J Chem Eng Data* 47:346–350
14. Chen CY, Cheng CT, Lai CW, Wu PW, Wu KC, Chou PT, Chou YH, Chiu HT (2006) Potassium ion recognition by 15-crown-5 functionalized CdSe/ZnS quantum dots in H_2O . *Chem Commun* 42:263–265
15. Ho ML, Hsieh JM, Lai CW, Peng HC, Kang CC, Wu IC, Lai CH, Chen YC, Chou PT (2009) 15-crown-5 functionalized Au nanoparticles synthesized via single molecule exchange on silica nanoparticles: its application to probe 15-crown-5/ K^+ /15-crown-5 “sandwiches” as linking mechanisms. *J Phys Chem C* 113:1686–1693
16. Patel G, Kumar A, Pal U, Menon S (2009) Potassium ion recognition by facile dithiocarbamate assembly of benzo-15-crown-5–gold nanoparticles. *Chem Commun* 45:1849–1851
17. Lin SY, Liu SW, Lin CM, Chen CH (2002) Recognition of potassium ion in water by 15-crown-5 functionalized gold nanoparticles. *Anal Chem* 74:330–335
18. Lin SY, Chen CH, Lin MC, Hsu HF (2005) A cooperative effect of bifunctionalized nanoparticles on recognition: sensing alkali ions by crown and carboxylate moieties in aqueous media. *Anal Chem* 77:4821–4828
19. Velu R, Ramakrishnan VT, Ramamurthy P (2010) Colorimetric and fluorometric chemosensors for selective signaling toward Ca^{2+} and Mg^{2+} by aza-crown ether acridinedione-functionalized gold nanoparticles. *Tetrahedron Lett* 51:4331–4335
20. Frens G (1973) Controlled nucleation for the regulation of the particle size in monodisperse gold suspensions. *Nat Phys Sci* 241:20–22
21. Anandhakumar S, Mathiyarasu J (2013) Detection of lead (II) using an glassy carbon electrode modified with Nafion, carbon nanotubes and benzo-18-crown-6. *Microchim Acta* 180:1065–1071
22. Späth A, König B (2010) Molecular recognition of organic ammonium ions in solution using synthetic receptors. *Beilstein J Org Chem* 6:1–111
23. Kuang H, Chen W, Yan W, Xu L, Zhu Y, Liu L, Chu H, Peng C, Wang L, Kotov NA, Xu C (2011) Crown ether assembly of gold nanoparticles: melamine sensor. *Biosens Bioelectron* 26:2032–2037
24. Flink S, Veggel FCJM, Reinhoudt DN (1999) Recognition of cations by self-assembled monolayers of crown ethers. *J Phys Chem B* 103:6515–6520
25. Pedersen CJ (1988) The discovery of crown ethers (Noble lecture). *Angew Chem Int Ed* 27:1021–1027
26. Jackson ML (1985) In soil chemical analysis. Parallel press, Wisconsin
27. Wei F, Lam R, Cheng S, Lu S, Ho D, Li N (2010) Rapid detection of melamine in whole milk mediated by unmodified gold nanoparticles. *Appl Phys Lett* 96:133702–133703
28. Lin CY, Yu CJ, Lin YH, Tseng WL (2010) Colorimetric sensing of silver (I) and mercury (II) ions based on an assembly of tween 20-stabilized gold nanoparticles. *Anal Chem* 82:6830–6837
29. Miao XM, Ling LS, Shuai XT (2012) Detection of Pb^{2+} at attomole levels by using dynamic light scattering and unmodified gold nanoparticles. *Anal Biochem* 421:582–586
30. Jiang C, Ma M, Wang Y (2012) Using gallic acid-modified gold nanoassemblies to detect the Pb^{2+} of tea. *Anal Methods* 4:3570–3574
31. Zhang Y, Leng Y, Miao L, Xin J, Wu A (2013) The colorimetric detection of Pb^{2+} by using sodium thiosulfate and hexadecyl trimethyl ammonium bromide modified gold nanoparticles. *Dalton Trans* 42:5485–5490
32. Guo Y, Wang Z, Qu W, Shao H, Jiang X (2011) Colorimetric detection of mercury, lead and copper ions simultaneously using protein-functionalized gold nanoparticles. *Biosens Bioelectron* 26:4064–4069
33. Cao H, Wei M, Chen Z, Huang Y (2013) Dithiocarbamate-capped silver nanoparticles as a resonance light scattering probe for simultaneous detection of lead (II) ions and cysteine. *Analyst* 138:2420–2426
34. Qi L, Shang Y, Wu F (2012) Colorimetric detection of lead (II) based on silver nanoparticles capped with iminodiacetic acid. *Microchim Acta* 178:221–227
35. Zhang L, Yao Y, Shan J, Li H (2011) Lead (II) ion detection in surface water with pM sensitivity using aza-crown-ether-modified silver nanoparticles via dynamic light scattering. *Nanotechnology* 27:275504